Central European Journal of Energetic Materials
ISSN 1733-7178; e-ISSN 2353-1843

Cent. Eur. J. Energ. Mater. 2019, *16*(4): 487-503; DOI 10.22211/cejem/112471
Article is available in PDF-format, in colour, at:
http://www.wydawnictwa.ipo.waw.pl/cejem/Vol-16-Number-4-2019/CEJEM_01085.pdf

Research paper

Detonation Parameters of PlSEM Plastic Explosive

Aline Cardoso Anastacio[1], **Jakub Selesovsky**[2], **Martin Künzel**[3], **Jindrich Kucera**[2], **Jiri Pachman**[2,*]

[1] *Military Institute of Engineering, Praça General Tibúrcio 80, 22290-270, Rio de Janeiro, Brazil*
[2] *Institute of Energetic Materials, Faculty of Chemical Technology, University of Pardubice, Studentska 95, CZ53210 Pardubice, Czech Republic*
[3] *OZM Research, s.r.o., Blížňovice 32, CZ53862 Hrochův Týnec, Czech Republic*
[*] *E-mail:* jiri@pachman.eu

Abstract: PlSEM is a plastic explosive based on RDX, PETN and a non-explosive binder, and is used in linear shaped charges for demolition purposes. Its experimentally obtained detonation parameters are presented in the present paper. The detonation velocity was measured for cylindrical charges of various diameters, with and without confinement. The detonation pressure and particle velocity were determined using an impedance window matching technique, and cylinder tests were used to obtain the parameters of the JWL equation of state of the detonation products. Detonation velocities from 7.75 to 8.05 km·s^{-1} were obtained for unconfined charges with diameters from 4 to 8 mm, and from 8.15 to 8.24 km·s^{-1} for charges with 25 mm diameter. The experimentally determined detonation pressure was found to be 24.6 GPa.

Keywords: detonation velocity, PlSEM, plastic explosive, detonation pressure, cylinder test

1 Introduction

The plastic explosive PlSEM is a commercial product of Explosia Company. It is produced in various shapes, including long A-shaped rods used in linear shaped charges for demolition work. It contains hexogen (RDX), pentaerythritol tetranitrate (PETN) and a non-explosive binder [1]. The reason for mixing the two explosive compounds is purely practical. The presence of PETN increases the sensitivity of the explosive and ensures reliable initiation by a standard industrial detonator, equivalent to a number 8 detonator, while the RDX improves the detonation parameters.

Although the detonation properties of RDX and PETN have already been extensively investigated [2-4], those of PlSEM explosive are not available. Detonation parameters refer to the state at the detonation front, normally reported at the Chapman-Jouguet plane (CJ), and include detonation velocity (D), density (ρ), detonation pressure (P), particle velocity (u) and energy (E) [3]. The detonation parameters, together with the equation of state (EOS) of the detonation products are required to model the explosive effects in various applications.

The detonation velocity D is relatively easily measured by various techniques [5]. Among others, optical methods have the advantage of high temporal resolution, robustness, low cost of consumables and increased safety, since no electrical signal is used for the measuring probes. The detonation velocity is known to be influenced by charge diameter and confinement [6, 7].

While it is relatively easy to measure D, this is not the case for detonation pressure (P_{CJ}), which is sometimes presented only as a result of calculations. The P_{CJ} can be measured directly from gauges embedded in the explosive [8], or by the measurement of a property of the shock wave induced by the detonation wave in material adjacent to the explosive. The particle velocity or the shock velocity are often the parameters of choice and are measured using arrays of electrical pins [9] or laser interferometric techniques including Fabry-Perot [10], VISAR [11] and Photonic Doppler velocimetry (PDV) [12]. The impedance window matching (IWM) approach, used in this work to determine the u_{CJ} and P_{CJ} of PlSEM, relies on PDV to measure the particle velocity at the interface between the explosive charge and a transparent inert window coated with a reflective material [13-15]. This approach offers the advantage of being non-invasive, as no gauges need to be inserted in the explosive and thus preventing disruption of the detonation wave. The method is furthermore fast enough to enable the determination of the detonation wave shape needed for a reasonably well resolved determination of the detonation pressure in the CJ plane.

The expansion of the detonation products can be mathematically described by various EOS: polytropic expansion law, Lennard-Jones-Devonshire (LJD), Becker-Kistiakowsky-Wilson (BKW), Jones-Wilkins-Lee (JWL), among others [16]. The JWL EOS [17] is experimentally obtained from so called cylinders tests [4, 16-20], in which the explosive being investigated is placed inside a metal cylindrical tube, usually made of copper, and the expansion of the cylinder walls upon detonation is measured [16, 21]. Streak or high-speed cameras can be used to measure the wall position with time, from which the expansion is normally derived by an analysis of the recordings [22, 23]. Alternatively the test can be instrumented with diagnostic techniques able to measure the wall velocity, such as the above mentioned contact pins or interferometric techniques including PDV [23-25]. The latter outperform the other techniques in temporal resolution, which is important especially in the early stages of the expansion where shock reverberations play a major role.

In the present paper, we report and discuss the experimentally obtained detonation parameters of PlSEM explosive, in terms of D, P and u at the CJ point. The detonation velocity was determined for confined and unconfined charges of several diameters. The detonation pressure and the particle velocity at the CJ were obtained by IWM, and the JWL EOS parameters of the expanding detonation products were experimentally determined by PDV and a high speed framing camera.

2 Materials and Methods

2.1 Materials

The plastic explosive PlSEM contained 25% of PETN, 63% of RDX and 12% of a binder based on polyisobutene, by mass. The uncased explosive charges used in this work were prepared by screw-extruding the explosive into long cylindrical rods of various diameters and lengths as shown in Table 1.

Table 1. Diameters, densities and length of uncased PlSEM charges

Nominal diameter [mm]	Diameter [mm]	Density [g·cm^{-3}]	Length [mm]
25	24.80 ±0.07	1.59 ±0.01	80.5 ±0.5
8	8.28 ±0.08	1.55 ±0.03	394.7 ±0.5
6	6.58 ±0.04	1.51 ±0.02	394.0 ±0.5
4	4.06 ±0.02	1.60 ±0.01	394.0 ±0.5

The confined charges were prepared by screw extruding 194 g of PlSEM into copper cylinders of length 250 mm. Loading of the plastic explosive into metal tubes is a technically challenging problem. Piecewise loading with sequential compression does not provide good homogeneity of the charge. The copper pipe was therefore attached to the head of the screw extruder, steam heated and the explosive was then pushed through the pipe to fill it. The charges obtained in this way were homogeneous with density 1.586 ±0.01 g·cm^{-3} and the explosive filled the entire internal volume of the cylinder with external diameter 29.87 mm and internal diameter 24.86 mm.

2.2 Detonation velocity determination

A passive optical method, employing standard telecommunication multimode optical fibres in contact with the charge, was used to capture the light from the detonation wave as it arrived at the fibre positions. The light intensity *vs.* time was recorded by a device (OPTIMEX, commercialized by OZM Research), with a time resolution of 4 ns. The arrival of the detonation wave at a fibre's position was taken as the time when the light intensity rose steeply [26]. The detonation velocity could then be determined as the slope of the correlation between the times of arrival and the positions of the fibres. Figure 1 shows an example of a detonation velocity setup for an unconfined charge, with the fibres, touching the surface of the bare explosive charge, held in position by a 3-D printed plastic holder (in grey). For the charges with diameters less than 25 mm, a booster of 5 g of Semtex 1A (a PETN based plastic explosive) was used to avoid initiation problems. The centring detonator holder, made of PU foam, is seen in Figure 1. The probes (fibres) were evenly spaced from the beginning of the charge to its end to capture the initial transients.

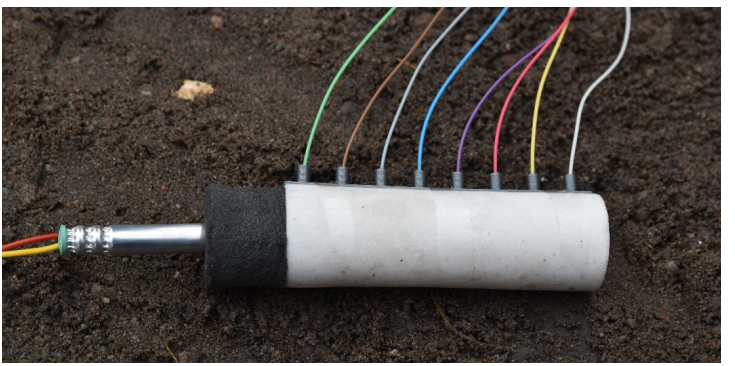

Figure 1. An example of the experimental setup used for measurement of the detonation velocity of an uncased charge

2.3 Detonation pressure determination

The impedance window matching technique was used to measure the detonation pressure of PlSEM, in an arrangement similar to that used for the detonation pressure measurement of RDX pressed charges [15]. The setup consisted of a 25 µm thick aluminium foil sandwiched between the flat surface of a cylindrical charge of PlSEM and a 10 mm thick polymethylmethacrylate (PMMA) window. A PDV probe aligned to the centre of the charge captured the velocities of the interface between the explosive and the PMMA window. The foil acted only as a reflective surface since the explosive itself is not reflective, and as it was very thin, the estimated shock reverberation was short (about 4 ns) and did not affect the overall signal. Figure 2 shows a schematic (a) and an image (b) of the setup.

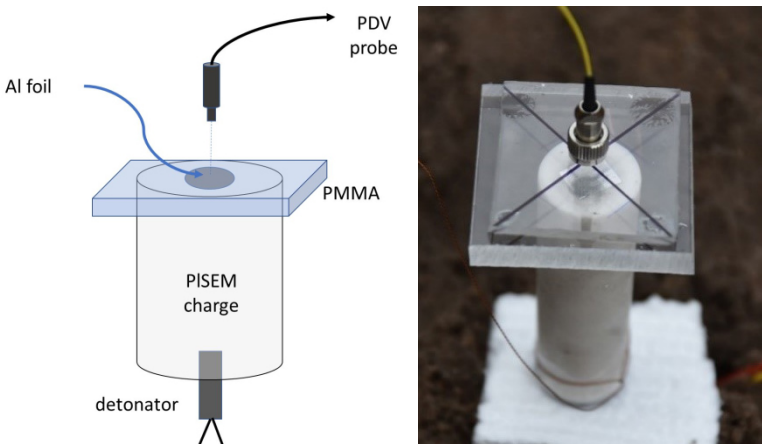

(a) (b)

Figure 2. Schematic (a) and photograph (b) of the detonation pressure measurements

The PDV system used in these experiments was produced by OZM Research. It employed a 1550 nm laser with power of 36 mW (for all channels). The signals were recorded on an oscilloscope (Tektronix DPO 70404) and were evaluated using a short time Fourier transform with Hanning window to obtain the velocity of the explosive–PMMA interface.

2.4 Cylinder tests

Three properties of the PlSEM explosive were obtained from the cylinder tests – detonation velocity, cylinder wall velocity and cylinder expansion.

The experimental setup is shown in Figure 3, as a schematic drawing (a) and photograph (b).

2.4.1. Detonation velocity in copper confinement

The same passive optical method as used in the determination of *D* in the uncased charges was applied in the tests of confined charges. The optical fibres were placed at 30, 130, 150, 170, 190 and 210 mm from the top of the charge (the detonator end), in holes drilled 2 mm into the copper (therefore not touching the explosive, since the cylinder wall was 2.5 mm thick).

2.4.2. Cylinder wall velocity

PDV was used to obtain the cylinder wall velocity history. Two collimator probes were placed at approximately 6 cm from the cylinder wall and inclined 5° to the horizontal, at heights corresponding to 130 and 150 mm from the top of the cylinder. The radial component of a copper wall particle velocity was used to obtain the JWL equation of state of the detonation products of PlSEM. The decomposition of the copper wall velocity (as measured by PDV) to obtain its radial component was done according to [24].

2.4.3. Cylinder wall expansion

A high-speed framing camera UHSi 12/24 by Invisible Vision Ltd, with lenses of 800 mm f/8, was used to record the cylinder wall expansion. The camera delay was set to 10 μs, the exposure time was 200 ns, and the frame rate was 400 000 fps. A 1.5 L bottle filled with argon was detonated near the charge using plastic explosive Semtex 1A to provide enough light for the camera recordings. The camera results consisted of a sequence of 12 frames showing the cylinder walls at different times, and consequently at different expansions. To capture all levels of expansion, two or more frames were manually overlapped, and this composition of frames was analysed by an edge function (with Lindemberg and threshold 5 options) using GNU/Octave software [27] to identify the edges of the tube. The edge positions in pixels were then converted into distances, using a pre-shot image as a reference for calibration. The result was a curve of radial wall position by longitudinal position in the cylinder, which could be converted into time by dividing it by the detonation velocity. This automated extraction of the cylinder expansion from the composition of the frames minimizes errors due to subjectivity. The radial wall velocity was obtained by taking the radial position *vs.* time data, fitting it by an equation (proposed by [28]) and differentiating this equation in time.

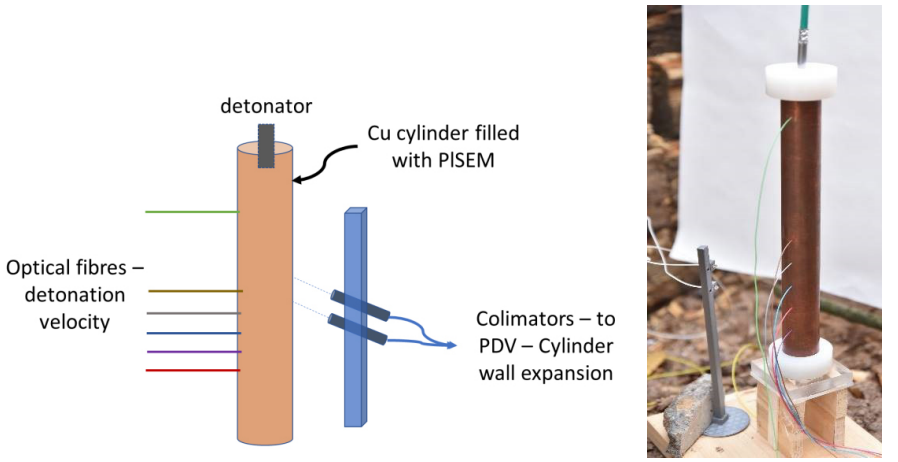

(a) (b)

Figure 3. Schematic (a) and photograph (b) of the cylinder tests setup

3 Results

3.1 Detonation velocity

Figure 4 shows an example of (a) the signals obtained in one of the shots, and (b) a close-up view of the signal with significant points related to the arrival time determination shown by an arrow. The fits of the detonation wave position *vs.* arrival time for some of the tested charges, with diameters of 4 to 25 mm, are shown in Figure 5. The error bars represent the uncertainty in the time of arrival determination.

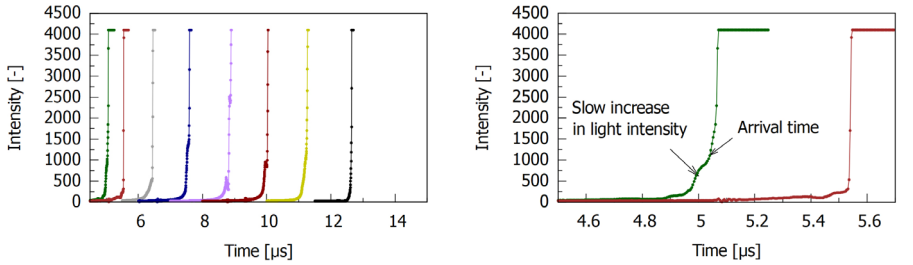

(a) (b)

Figure 4. Example of (a) an optical signal with 8 probes, and (b) detail of the time of arrival determination for the first two probes. The non-relevant part of the signal was cut-off for clarity

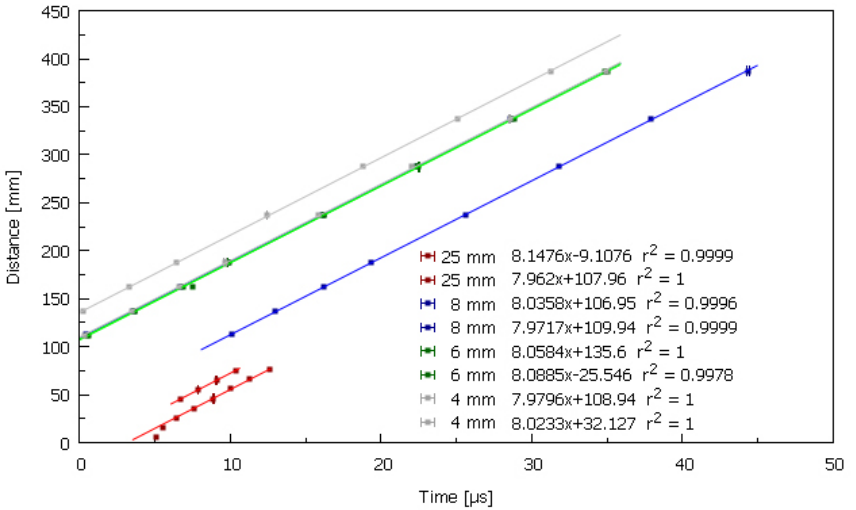

Figure 5. Distance of probes *vs*. time for several uncased charges, with different diameters

The value of *D* was determined from the slope of the fits of distance *vs.* time shown in Figure 5. In one of the charges with 25 mm diameter, the first point (corresponding to the probe closest to the detonator) was excluded from the fit, as it was anticipated to be affected by the initiation transients. The summary of the detonation velocity variation with the reciprocal charge diameters is shown in Figure 6 for all of the shots. The detonation velocity ranged from 7.75 to 8.05 km·s^{-1} for the charges with diameters from 4 to 8 mm; no obvious trend was observed within this range of diameters. One of the smaller diameter charges had a considerably lower detonation velocity, for no obvious reason. The 25 mm diameter charges had a slightly higher detonation velocity compared to the 4 and 8 mm diameter ones, ranging from 8.15 to 8.24 km·s^{-1}. The confined charges with 25 mm diameter had about the same detonation velocity as the uncased ones.

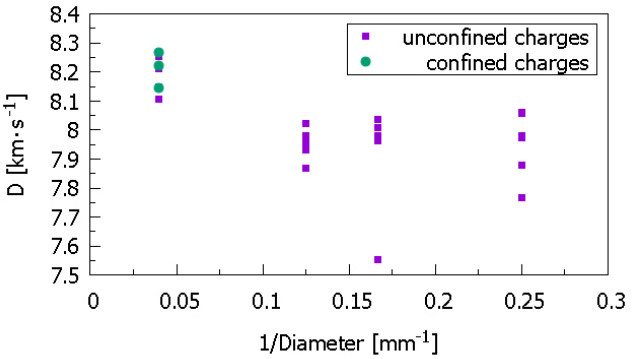

Figure 6. Dependence of the detonation velocity of PlSEM explosive on the charge diameter

3.2 Detonation pressure

Figure 7 shows an example of a successfully obtained spectrogram, corresponding to the velocities of the interface between PlSEM and PMMA, and includes an example of the analysis for the determination of the u_{PMMA}.

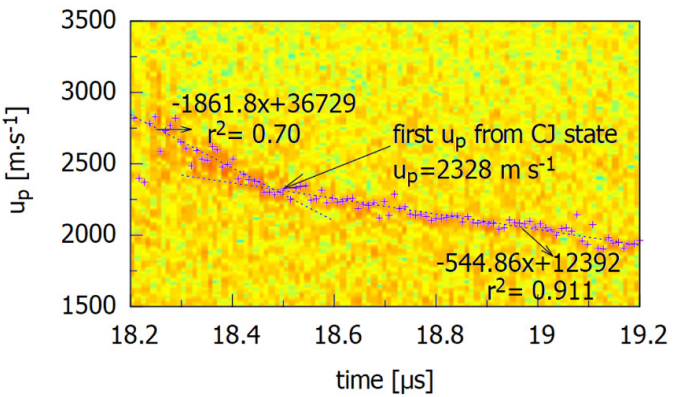

Figure 7. Example of a spectrogram showing velocities *vs*. time obtained with an IWM experiment for PlSEM explosive

The earlier part of the velocities measured for the PMMA corresponds to the von Neumann spike, which is then attenuated to the CJ state later attenuated by the Taylor wave. The point in the signal corresponding to the state transmitted by the CJ state can therefore be determined as the point where these two decreasing velocity trends intersect. In the approach used

by [15], these two trends were fitted by two straight lines, and the particle velocity in the transmitted CJ state ($u_{\text{expl-PMMA}}$) was taken as the experimental point closest to the intersection of the two lines. The detonation pressure (P_{CJ}) was then derived from $u_{\text{expl-PMMA}}$ by impedance matching, as shown in Figure 8, which displays the PMMA shock Hugoniot, the detonation Rayleigh line and the EOS for the detonation products in the $P - u$ plane. The CJ state is determined as the intercept of the detonation products EOS and the Rayleigh line.

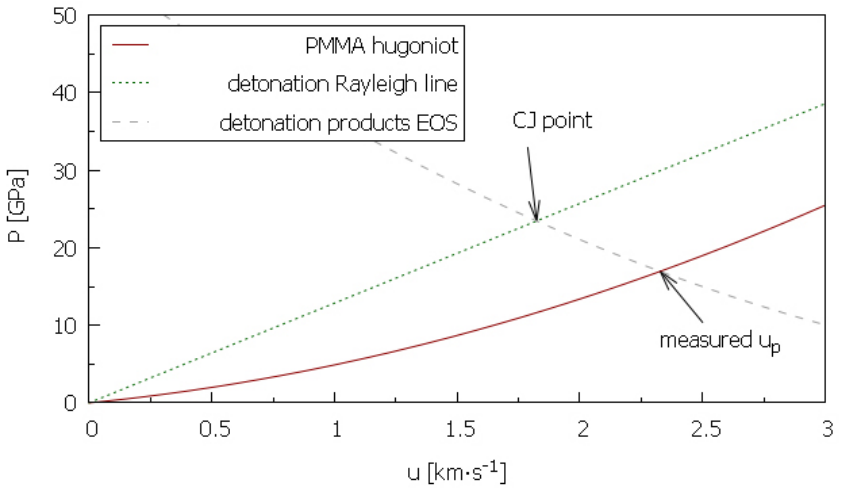

Figure 8. Impedance matching diagram for the experiment

In the plot of Figure 8, the Rayleigh line is known (because the detonation velocity has been previously measured), the PMMA Hugoniot is also known from the literature [29] and the only unknown needed to determine the CJ state of the detonation is the reacted explosive EOS, approximated to by the generalised EOS proposed by [3], and given by:

$$\frac{P}{P_{CJ}} = 2.412 - 1.7315\frac{u}{u_{CJ}} + 0.3195\frac{u}{u_{CJ}}^{2} \tag{1}$$

This EOS is a function of P_{CJ} and u_{CJ}, and, as it represents the states of the detonation products, it passes through the state measured by the PDV at the interface with the PMMA window. This condition and the fact that the CJ state also belongs to the Rayleigh line, provide the number of equations needed to solve the problem for P_{CJ} and u_{CJ}, obtained as 23.45 GPa and 1.824 km·s^{-1} for one of the shots and 25.65 GPa and 1.996 km·s^{-1} for a second shot.

3.3 Cylinder tests

The wall velocity histories obtained by PDV during the cylinder tests (left axis) are shown in Figure 9, which also includes the correspondent ratio of expansion (right axis). The early part of the signals shows the reverberations in the wall, which happens when the cylinder material has a speed of sound lower than the detonation velocity. One of the signals (shown in red) had significantly lower velocities following the forth reverberation. It is possible that a slight difference in the wall thickness between these shots, in the region of the cylinder covered by the laser, was responsible for the discrepancy.

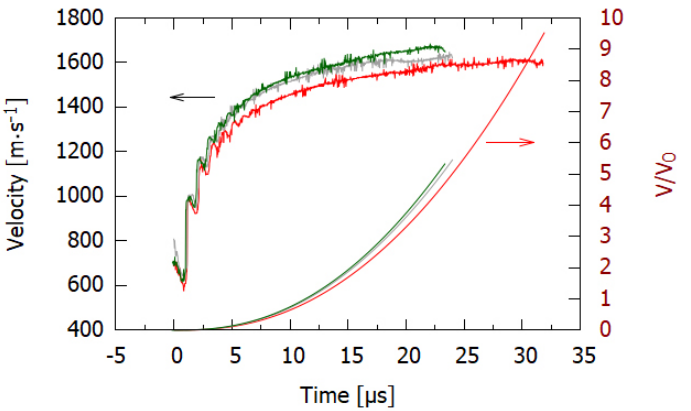

Figure 9. Results of the PDV measurements of the cylinder wall velocity (left axis) and the corresponding volumetric ratio of expansion (right axis) for three identical shots

The cylinder expansion was also measured by high-speed camera, and Figure 10(a) shows an example of a composition of two frames obtained. Figures 10(b) and 10(c) correspond to the same composition after edge recognition (Figure 10(b)) and Figure 10(c) – the overlap between Figure 10(a) and Figure 10(b) – shows good agreement between the two.

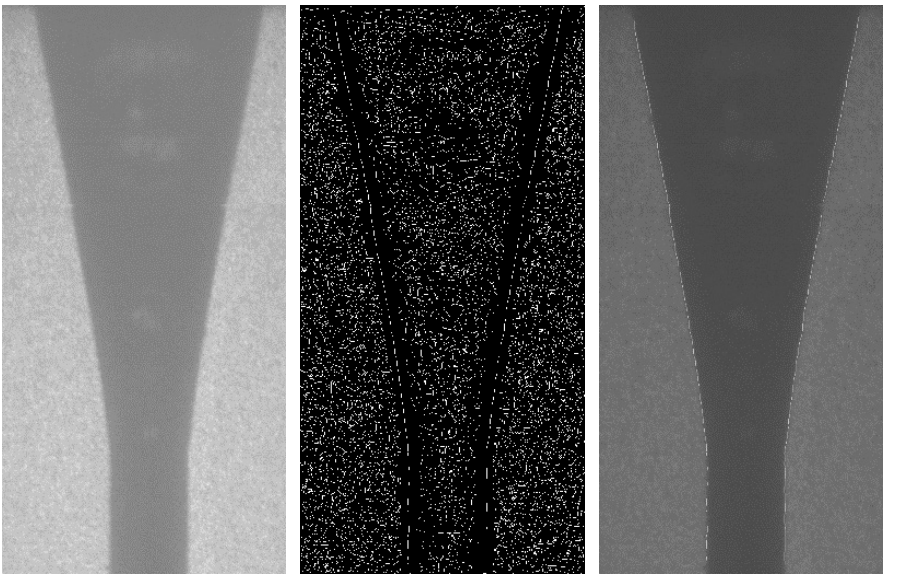

(a) (b) (c)

Figure 10. Three stages of the expansion extraction from the high-speed camera frames: (a) frame from the high-speed camera, (b) frame after edge extraction, using software and (c) overlapped Figures 10(a) and 10(b)

After being extracted and treated according to the procedure cited in the experimental section, the cylinder expansion was compared to the data obtained from the PDV, as shown in Figure 11, showing that the camera and PDV results agreed reasonably well, with the camera giving only slightly lower parameters. It can also be noted that the velocities obtained from the camera measurements are smooth, not reproducing the shock reverberations in the cylinder wall, as it is the derivative of an already smooth function.

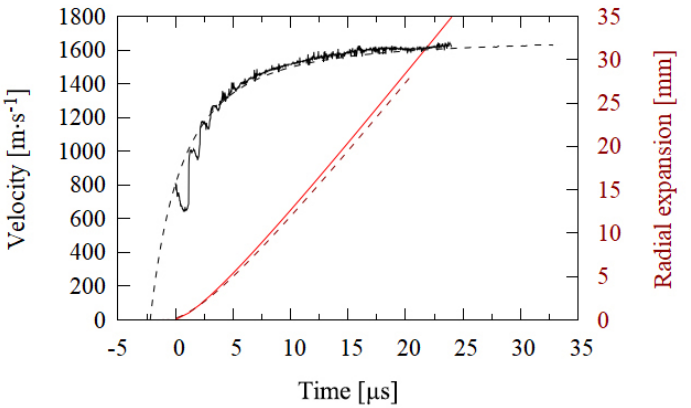

Figure 11. Comparison between camera and PDV results for the wall radial velocity (black curve – left axis) and the wall radial displacement (red curve – right axis) for one of the shots. Dashed lines correspond to camera data

3.3.1 JWL determination

The PDV data were used to obtain a JWL equation of state, employing the approach described in [23] and neglecting the corrections for heat losses, spall and airgaps (since the explosive was pressed directly into the tubes). The experimentally determined density (d = 1.58 g·cm^{-3}), detonation velocity (D = 8290 m·s^{-1}) and detonation pressure (P = 24.6 GPa) were used as the input values. The isentrope obtained is shown in Figure 12, and the JWL parameters are listed in Table2. A detonation energy of 5.5 MJ·kg^{-1} was determined from the area between the Rayleigh line and the EOS for a final relative expansion of 7.

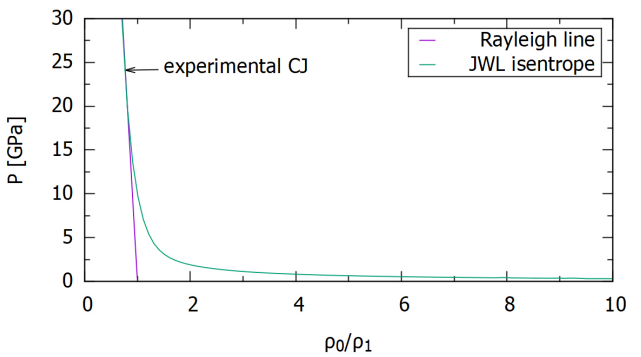

Figure 12. Experimental Rayleigh line and JWL isentrope

Table 2. JWL parameters for PlSEM

JWL parameter	Unit	Experimentally obtained value
A	[GPa]	962.21
B	[GPa]	5.5423
C	[GPa]	1.8553
R1	–	5.0004
R2	–	1.4667
E0	[kJ·cm^{-3}]	7.0070
w	–	0.45821
D	[m·s^{-1}]	8290
P_CJ	[GPa]	24.6
d	[g·cm^{-3}]	1.58

A simulation of the cylinder wall expansion was carried out as a 2D axisymmetric Eulerian with a mesh size 0.2 mm using LS-DYNA (version smp s R8.1.0, revision 105896). The air was described as an ideal gas, the explosive was characterized as a high explosive burn material and JWL EOS, with the constants obtained from the experimental cylinder shot. The copper tube was described with the Johnson-Cook material model and a linear polynomial EOS. The comparison between the experimental data (measured by PDV) and the velocity profile obtained from the simulation is shown in Figure 13. A good agreement can be observed between the simulation and the data, indicating that the JWL obtained can represent the expansion of the detonation products during the cylinder tests.

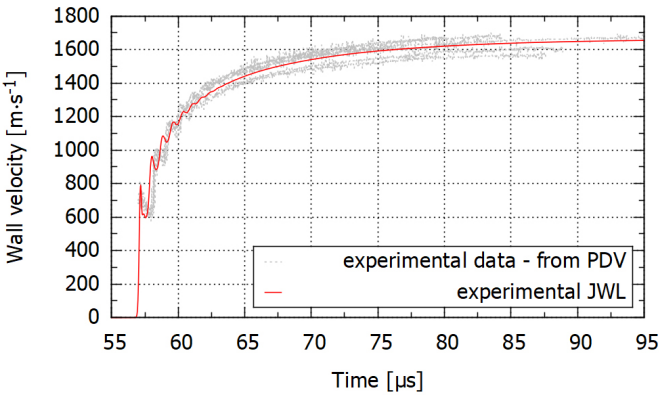

Figure 13. Comparison of LS-DYNA simulation based on experimentally determined JWL parameters (red line) with experimental PDV data (grey lines)

4 Conclusions

The detonation parameters of the plastic explosive PlSEM are presented. The detonation velocity was measured in both unconfined and confined cylindrical charges, for several diameters. The values of the detonation velocity were about the same for diameters in the range 4 to 8 mm, and slightly higher for charges with 25 mm diameter, with no obvious difference in the value of *D* due to charge confinement.

The detonation pressure was measured using an impedance window matching technique, and an average value of 24.6 GPa was obtained. Cylinder tests were performed, and the expansion of the cylinder wall was tracked by PDV and high-speed camera technique. The camera evaluation was done by a semi-automated approach, and both camera and PDV provided similar results. The expansion of the cylinder wall measured by PDV was used to obtain the JWL equation of state of the explosive, which was then used to simulate the cylinder test, with good agreement with the experimental data.

Acknowledgements

This work was supported by the University of Pardubice grant SGS_2019_002. We would further like to thank the Research Institute of Industrial Chemistry, Explosia Ltd., Czech Republic, especially Ladislav Riha for preparing the explosive charges.

References

[1] Explosia. [Online available: https://explosia.cz/app/uploads/2016/03/pisem.pdf (Accessed: 21-JUN-2019)].
[2] Chirat, R.; Pittion-Rossillon, G.A. New Equation of State for Detonation Products. *J. Chem. Phys.* **1981**, *74*(8): 4634.
[3] Cooper, P.W. *Explosives Engineering.* Wiley-VCH Inc., New York, **1996**; ISBN 0-471-18636-8.
[4] Baudin, G.; Serradeill, R. Review of Jones-Wilkins-Lee Equation of State. *EPJ Web Conf.* **2010**, *10*: 00021.
[5] Tete, A.D.; Deshmukh, A.Y.; Yerpude; R.R. Velocity of Detonation (VOD) Measurement Techniques – Practical Approach. *Int. J. Eng. Techn*. **2013**, *2*(3): 259-265.
[6] Eyring, H; Powell, R.E.; Duffey, G.E.; Parlin R.B. The Stability of Detonation. *Chem. Rev.* **1949**, *45*(1): 69-181.
[7] Souers, P.C.; Vitello, P.; Esen, S.; Kruttschnitt, J.; Bilgin, H.A. The Effects of

Containment on Detonation Velocity. *Propellants Explos. Pyrotech.* **2004**, *29*(1): 19-26.

[8] Vantine, H.; Chan, J.; Erickson, L.; Janzen, J.; Weingart, R.; Lee, R. Precision Stress Measurements in Severe Shock-Wave Environments with Low-Impedance Manganin Gauges. *Rev. Sci. Instrum.* **1980**, *51*(1): 116-122.

[9] Duff, R.E.; Houston, E. Measurement of the Chapman-Jouguet Pressure and Reaction Zone Length in a Detonating High Explosive. *J. Chem. Phys.* **1955**, *23*(7): 1268-1273.

[10] Fedorov, A.V.; Mikhailov, A.L.; Antonyuk, L.K.; Nazarov, D.V.; Finyushin, S.A. Determination of Chemical Reaction Zone Parameters, Neumann Peak Parameters, and the State in the Chapman-Jouguet Plane in Homogeneous and Heterogeneous High Explosives. *Combust. Explos. Shock Waves* **2012**, *48*(3): 302-308.

[11] Bouyer, V.; Doucet, M.; Decaris, L. Experimental Measurements of the Detonation Wave Profile in a TATB Based Explosive. *EPJ Web Conf*. **2010**, *10*: 00030.

[12] Lorenz, K.T.; Lee, E.L.; Chambers, R. A Simple and Rapid Evaluation of Explosive Performance – the Disc Acceleration Experiment. *Propellants Explos. Pyrotech*. **2015**, *40*(1): 95-108.

[13] Gustavsen, R.L.; Bartram, B.D.; Sanchez, N. Shock Initiation Measurements using Multiple Samples Instrumented with PDV. *Annual Photonic Doppler Velocimetry Workshop*, *4th,* Austin, Texas, **2009**.

[14] Sheffield, S.A.; Bloomquist, D.D.; Tarver, C.M. Subnanosecond Measurements of Detonation Fronts in Solid High Explosives. *J. Chem. Phys.* **1984**, *80*(8): 3831-3844.

[15] Pachman, J.; Künzel, M.; Němec, O.; Majzlík, J. A Comparison of Methods for Detonation Pressure Measurement. *Shock Waves* **2017**, *28*(2): 207-225.

[16] Davis, W.C. Shock Waves; Rarefaction Waves; Equations of State. In: *Explosive Effects and Applications* (Zukas, J.A.; Walters, W.P., Eds), Springer, New York, **1998**, pp. 47-114; ISBN 0-387-98201-9.

[17] Weseloh, W.N. *JWL in a Nutshell*. Los Alamos National Laboratory Report LA-UR-14-24318, **2014**.

[18] Elek, P.M.; Dzingalasevic, V.; Jaramaz, S.S.; Mickovic, D.M. Determination of Detonation Products' Equation of State from Cylinder Test: Analytical Model and Numerical Analysis. *Therm. Sci.* **2015**, *19*(1): 35-48.

[19] Merchant, P.W.; White, S.J.; Collyer, A.M. A WBL-Consistent JWL Equation of State for the HMX-Based Explosive EDC37 from Cylinder Tests. *Int. Det. Symp.*, *Proc., 12th,* San Diego, **2002**.

[20] Menikoff, R. Detonation Waves in PBX 9501. *Combust. Theor. Model.* **2006**, *10*(6): 1003-1021.

[21] Hornberg, H.; Volk, F. The Cylinder Test in the Context of Physical Detonation Measurement Methods. *Propellants Explos. Pyrotech*. **1989**, *14*(5): 199-211.

[22] Lindsay, C.M.; Butler, G.C.; Rumchik, C.G.; Schulze, B.; Gustafson, R.; Maines, W.R. Increasing the Utility of the Copper Cylinder Expansion Test. *Propellants Explos. Pyrotech*. **2010**, *35*(5): 433-439.

[23] Souers, P.C.; Vitello, P.A. *Detonation Energy Densities from the Cylinder Test.* Lawrence Livermore National Laboratory Report LLNL-TR-666420, **2015**.
[24] Jackson, S. The Detonation Cylinder Test: Determination of Full Wall Velocity and Shape from a Single Velocimetry Probe with an Arbitrary Angle. *AIP Conf., Proc.* **2017**, 1793: 50017.
[25] Briggs, M.E.; Hill, L.; Hull, L.; Shinas, M. *Applications and Principles of Photon Doppler Velocimetry for Explosives Testing*. Los Alamos National Laboratory Report 10-01427, **2010**.
[26] Pachman, J.; Künzel, M.; Kubat, K.; Selesovsky, J.; Marsalek, R.; Pospisil, M.; Kubicek, M.; Prokes, A. OPTIMEX: Measurement of Detonation Velocity with a Passive Optical Fibre System. *Cent. Eur. J. Energ. Mater.* **2017**, *14*(1): 233-250.
[27] Eaton, J.W.; Bateman, D.; Hauberg, S.; Wehbring, R. *GNU Octave Version 4.0.0 Manual: a High-Level Interactive Language for Numerical Computations.* **2015**, [Online available: http://www.gnu.org/software/octave/doc/interpreter/ (Accessed: 21-JUN-2019)].
[28] Hill, L.G.; Catanach, R.A. *W-76 PBX 9501 Cylinder Tests*. Los Alamos National Laboratory Report LA-13442-MS, **1998**.
[29] Marsh, S.P. *LASL Shock Hugoniot Data.* University of California Press, **1980**.

Received: July 12, 2019
Revised: September 19, 2019
First published online: December 20, 2019